

# Electronic Supporting Information: Comparative Study Demonstrates Strong Size Tunability of Carrier-Phonon Coupling in CdSe-Based 2D and 0D Nanocrystals

Riccardo Scott,<sup>†</sup> Anatol V. Prudnikau,<sup>‡,△</sup> Artsiom Antanovich,<sup>‡</sup> Sotirios  
Christodoulou,<sup>¶</sup> Thomas Riedl,<sup>§</sup> Guillaume H. V. Bertrand,<sup>||,⊥</sup> Nina  
Owschimikow,<sup>†</sup> Jörg K.N. Lindner,<sup>#</sup> Zeger Hens,<sup>@</sup> Iwan Moreels,<sup>@,⊥</sup> Mikhail  
Artemyev,<sup>‡</sup> Ulrike Woggon,<sup>†</sup> and Alexander W. Achtstein<sup>\*,†</sup>

<sup>†</sup>*Institute of Optics and Atomic Physics, Technical University of Berlin, Berlin, Germany*

<sup>‡</sup>*Research Institute for Physical Chemical Problems of Belarusian State University, Minsk,  
Belarus*

<sup>¶</sup>*ICFO-Institut de Ciències Fotoniques, Castelldefels, Spain*

<sup>§</sup>*Department of Physics, Paderborn University, Paderborn, Germany*

<sup>||</sup>*CEA Saclay, 91191 Gif-sur-Yvette, France*

<sup>⊥</sup>*Istituto Italiano di Tecnologia, Genova, Italy*

<sup>#</sup>*Department of Physics, Paderborn University, Paderborn, Germany*

<sup>@</sup>*Department of Chemistry, Ghent University, Ghent, Belgium*

<sup>△</sup>*Current address: Physical Chemistry, TU Dresden, Dresden, Germany*

E-mail: achtstein@tu-berlin.de

Fax: +49(0)30 31421079

# Exciton-Phonon Coupling

## Temperature dependent Bandgap

In the main text of the manuscript we used the exciton-phonon coupling strength  $a_{ep}$  together with a Bose model<sup>1,2</sup> for the temperature dependent bandgap

$$E_{max} = E_0 - a_{ep} \left( 1 + \frac{2}{e^{\theta/T} - 1} \right), \quad (\text{S1})$$

Using  $\coth(x) = 1 + 2/(e^{2x} - 1)$  and O'Donnell et al.<sup>2</sup> this equation is equivalent to an expression

$$E_{max} = E'_0 - S \langle \hbar\omega \rangle \coth \left[ \frac{\langle \hbar\omega \rangle}{2k_B T} \right] \quad (\text{S2})$$

using the dimensionless Huang-Rhys parameter  $S$ , the average phonon energy  $\langle \hbar\omega \rangle$  and the zero temperature bandgap  $E'_0$  including polaron shift. Using the exponential function representation it can be shown that the parameters in both model are inter related via  $\Theta = \langle \hbar\omega \rangle / k_B$  so that  $S = a_{ep} / k_B \Theta$ .  $S$  is also a measure for the exciton-phonon coupling strength. Using the fit results in Figures 2 and 3 of the main text, we are able to calculate the resulting  $S$ . Figure S1 shows the results for the core-only platelets and core-shell platelets and quantum dots. In line with Figure 2 and its discussion in the main text we observe an increase of the exciton-phonon coupling with increasing platelet size.

Figures S1 (b) and (c) also demonstrate that in line with the trends for  $a_{ep}$  the phonon coupling is reduced with increasing CdS shell thickness both in platelets and dots, apart from an outlier for the thickest CdS shell, which may be explained by the very low  $\Theta$  value in Figure 3 (f) (main text), as  $S$  scales with the inverse of  $\Theta$ . We remark that all obtained Huang-Rhys factors are averages over the phonon density of states containing both acoustic and optical modes and hence not easy to be compared with e.g. Raman measurements, as that technique is mode selective. The Huang-Rhys parameters obtained do not reflect the coupling of a single mode, but an average over optical and acoustic modes, which reflect

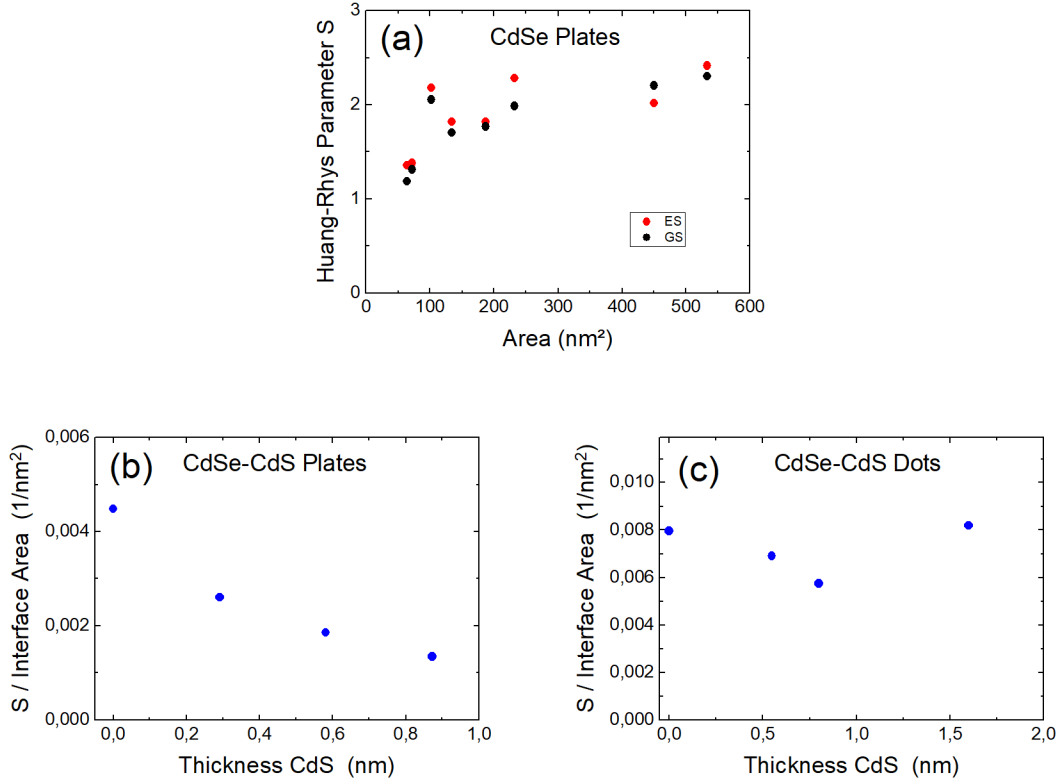


Figure S1: Huang Rhys factors as obtained from Equation S2 and the relations to S1 as well as the values in Figures 2 and 3 (main text) for CdSe core only (a) and CdSe-CdS (b) platelets as well as CdSe-CdS dots (c).

both bandgap shift by temperature dependent phonon progression as well as phonon induced lattice expansion due to nonparabolicity.<sup>2</sup>

Looking at the average phonon temperatures (Fig. 2 d) we see that both must have considerable contribution as  $\Theta$  is somewhere in-between the energies of LO and low energy acoustic modes. Kelley<sup>3</sup> showed for CdSe dots that the low energy (acoustic) modes ( $<100\text{cm}^{-1}$ ) have considerably higher Huang-Rhys factors as compared to optical modes. Hence it is not unexpected that the average S obtained in our manuscript may be higher as compared to the values for a single LO mode only. But there are no data available in literature (e.g. from Raman) yet.

It is further interesting to compare our obtained S values with other material systems. In MoS<sub>2</sub>, a transition metal dichalcogenide with mm lateral size monolayers,  $S = 1.87$  has been found,<sup>4</sup> for MoTe<sub>2</sub>  $S = 2.03$ .<sup>5</sup> Hence, our values for CdSe platelets in Figure S1 (a) are

in a similar range, substantiating our results.

## Energy scaling of CdSe platelet double emission

In Figure 2 (b) (main text) we analyze the impact of lateral confinement on the zero temperature excitonic bandgap of CdSe nanoplatelets. Starting from the approximate expression for the confinement energy related bandgap shift  $\Delta E$  of an infinitely deep semiconductor quantumbox in x, y and transversal z direction the observed bandgap is

$$E_g = E_{g,bulk} - E_B + \frac{n_z^2 \pi^2 \hbar^2}{2\mu_z L_z^2} + \frac{\pi^2 \hbar^2}{2M_{x,y}} \left[ \left( \frac{n_x}{L_x} \right)^2 + \left( \frac{n_y}{L_y} \right)^2 \right] \quad (S3)$$

with  $E_{g,bulk}$  the bulk bandgap,  $E_B$  the exciton binding energy,  $\mu$  the reduced exciton mass.  $M_{x,y}$  is the exciton mass and  $n_{x,y,z}$  the quantum number in x,y,z direction. We note that NPLs are strongly confined in z-direction (quantization of relative motion), while weakly confined in in-plane directions<sup>6</sup> (quantization of center of mass motion). Under the assumption of a lowest electron and hole state transition  $n_{x,y,z} = 1$  in all directions and taking the x-direction as the long side of the rectangular platelet, the first excited state would be  $(n_x, n_y, n_z) = (2, 1, 1)$  and the ground state  $(1, 1, 1)$ .

The exciton binding energy depends only weakly on the lateral size<sup>6</sup> and can be assumed to be constant. The first term in eq. S3, the CdSe bulk low temperature bandgap of 1.776 eV, as well as the well-width of the anisotropic quantumbox (4.5 ML) can also be considered constant in lateral size variation, so that we plot  $dE = E_g - E_{g,bulk} + E_B$  versus  $(1/L_x)^2 + (1/L_y)^2$ . Here we assume (1,1,1) for the upper and lower emission state from Figure 1 (main text) and observe a linear dependence fitted in this plot ( $R^2 = 0.98$ ). The offset is related to z-confinement, whereas the slope  $\pi^2 \hbar^2 / 2M_{x,y}$  corresponds to the quasi-particle (e.g. exciton) mass. The different slopes indicate different masses of the emitting species, inferring different species as the origin of the double emission, e.g. ground and excited state excitons, exciton and trion or exciton and biexciton. A plot under the assumption of ground state (GS) (1,1,1)

and excited state (ES) (2,1,1) excitons leads to less good correlation ( $R^2 = 0.94$ ) for a fit to the shifts vs.  $(n/L_x)^2 + (1/L_y)^2$  and is shown in the inset of Figure 2 (b). Note that for the same platelets ES and GS appear at different positions on the x-scale. However, a definite answer to which of the two models applies cannot be given based on the lateral confinement. In the following, we discuss the first case.

According to Equation S3 we find  $M_{ES} = 0.276 \pm 0.021 m_0$   $M_{GS} = 0.513 \pm 0.091 m_0$  obtained from the slopes in Figure 2 (b), so that the masses have the ratio  $M_{GS}/M_{ES} = 1.86$  (the indices do not presume any attribution to the nature of the two states). We can now compare this result with the in-plane masses of heavy-hole (hh) excitons, trions and biexcitons. Using Luttinger parameters from Refs. 7 and 6 and their relation to the in- and out-of-plane effective masses<sup>8</sup> as well as the definitions of the trion  $M^{X-} = 2m_e + m_h$  and biexciton mass  $M^{XX} = 2(m_e + m_h) = 2M^X$  we find  $M_{x,y}^X = 0.287 m_0$ ,  $M_{x,y}^{X-} = 0.407 m_0$  and  $M_{x,y}^{XX} = 0.574 m_0$  as predictions. These masses would produce a ratio for the lower to higher energetic state of  $M^{X-}/M^X = 1.12$ ,  $M^{X+}/M^X = 1.17$  and  $M^{XX}/M^X = 2.00$ . Considering that published electron masses for ZB CdSe vary already by 7 percent (0.12-0.13  $m_0$ ), the biexciton scenario comes closest to our experimentally obtained ratio of  $M_{GS}/M_{ES} = 1.86$  and could be an explanation for the low energy emission peak. Arguments for this attribution may be the lack of circular polarization of the low energy emission as compared to the higher energy peak (which we call ES), that shows clear circular polarization.<sup>9</sup> On the other hand, also a trion emission can show no circular polarization, so that this cannot be taken as an exclusive argument. In excitation power dependent PL experiments no quadratic excitation intensity dependence has been found.<sup>6</sup> However, it is known that under certain circumstances a biexciton can exhibit a linear power dependence.<sup>10</sup> There is also the possibility that if the first exciton stems from a long-lived dark exciton and only the second one from the actual excitation pulse, a linear power-dependence would be observed nonetheless. A final conclusion on the attribution of these two states is beyond the scope of this article, as the mass ratios do not allow a clear identification.

# Remarks on the impact of band alignment, inhomogeneous broadening and strain on line width

Band alignment: The band alignment in CdSe-CdS nanoplatelets can be shown to be type I, so that there is no formation of spatially indirect excitons (type I 1/2 or II), which is proved by calculations as well as time-resolved measurements, showing no alteration of the transition dipole moment.<sup>11</sup> We have also measured the time dependent dynamics of the nanoparticles (Ref. 11) and found that the radiative rates are practically unaltered comparing core only and core shell, and only the suppression of nonrad. recombination leads to an increase of the PL lifetime with shell thickness, what clearly supports the type I band alignment, as in type I 1/2 and II cases significant alterations of the radiative rates should occur. The type I band alignment is also in line with results in Ning et al.<sup>12</sup> and Wang et al.<sup>13</sup> (Fig. 4) for core-shell dots, so that both core-shell platelets and dots have the same band alignment. Therefore the emission is not broadened by type II band alignment.

Inhomogeneous broadening in dots and hetero interface induced strain: We remark that this can not affect the results obtained from the temperature dependent bandgap, and the from there derived coupling parameters.(Fig. 3 d,f). On the other hand we can decide whether inhom. broadening is a relevant effect in our core-shell dots for the deduction of the exciton-phonon coupling strength. Any inhom. broadening would affect only the zero temperature offset in equation (3), as it is temperature independent, but not the other two temperature dependent summands. However, only the latter two are relevant for the determination of the phonon coupling. So even if there is inhom. broadening, there will be no relevant impact on the determination of the phonon couplings from the line width plotted in Figure 3, as it is only an offset.

Also, we would like to point that strain, which might be introduced by a mismatch of the CdS and CdSe lattice parameters, will not result in broadening of the emission. For the

occurrence of broadening due to strain it is relevant that the extend of the strain field is bigger than the exciton Bohr radius. Only then excitons having their center of mass at different locations experience different lattice parameters and hence due to the local distortion of the bandgap a different transition energy, what results in an inhom. broadened emission. In the case of strong confinement, like in the 4 nm diam. dots the wavefunction is spread over the whole particle and hence any shell induced strain will not result in broadening of the emission. Hence our approach of extracting the phonon coupling from the temperature dependent contrib. to the line broadening is valid. Further we remark, that we can also exclude a relevant contribution due to strain in the core shell structure. If strain would be relevant for the (inhom.) line width, with increasing shell thickness we should observe an increase of the zero temperature spectral width with shell thickness, in contrast to the observations in Fig. 4 (g). So strain is not a dominant parameter in the system and our approach does not suffer from it. For the platelets the excitons are coherently delocalized over the whole platelet, what for example causes the Giant Oscillator Strength effect related increase of the PL lifetime with temperature.<sup>14</sup> Hence there will be no inhom. broadening due to strain in the nanoplatelets, as the excitons averages over the whole platelet.

We further remark with regard to to the impact of non-radiative decay channels that they are not really relevant for the homogeneous line width, as it is well established that in CdSe based nanoparticles (with reasonable quantum yield ( $>10\%$  for all samples here)) the pure dephasing (which is related to decoherence by phonon scattering) is always considerably greater as compared to all radiative and non radiative decay contributions. The system is pure dephasing limited as the  $T_2$  time is considerably lower than the population decay time  $T_1$ .<sup>15</sup> The discussions above clearly justify our approach in the manuscript, and rules out any obstacle by the mentioned effects.

## References

1. Vina, L.; Logothetidis, S.; Cardona, M. Temperature dependence of the dielectric function of germanium. *Phys. Rev. B* **1984**, *30*, 1979–1991.
2. O'Donnell, K. P.; Chen, X. Temperature dependence of semiconductor band gaps. *Appl. Phys. Lett.* **1991**, *58*, 2924–2926.
3. Kelley, A. M. Electron-Phonon Coupling in CdSe Nanocrystals from an Atomistic Phonon Model. *ACS Nano* **2011**, *5*, 5254–5262.
4. Cadiz, F.; Courtade, E.; Robert, C.; Wang, G.; Shen, Y.; Cai, H.; Taniguchi, T.; Watanabe, K.; Carrere, H.; Lagarde, D.; Manca, M.; Amand, T.; Renucci, P.; Tongay, S.; Marie, X.; Urbaszek, B. Excitonic Linewidth Approaching the Homogeneous Limit in MoS<sub>2</sub>-Based van der Waals Heterostructures. *Phys. Rev. X* **2017**, *7*, 021026.
5. Helmrich, S.; Schneider, R.; Achtstein, A. W.; Arora, A.; Herzog, B.; de Vasconcelos, S. M.; Kolarczik, M.; Schoeps, O.; Bratschitsch, R.; Woggon, U.; Owschimikow, N. Exciton phonon coupling in mono- and bilayer MoTe<sub>2</sub>. *2D Materials* **2018**, *5*, 045007.
6. Achtstein, A. W.; Scott, R.; Kickhöfel, S.; Jagsch, S. T.; Christodoulou, S.; Bertrand, G. H.; Prudnikau, A. V.; Antanovich, A.; Artemyev, M.; Moreels, I.; Schliwa, A.; Woggon, U. p-State Luminescence in CdSe Nanoplatelets: Role of Lateral Confinement and a Longitudinal Optical Phonon Bottleneck. *Phys. Rev. Lett.* **2016**, *116*, 116802.
7. Willatzen, M.; Cardona, M. Spin-orbit coupling parameters and electron g factor of II-VI zinc-blende materials. *Phys. Rev. B* **1995**, *51*, 992–994.
8. Basu, B. K. *Theory of Optical Processes in Semiconductors*; Oxford Univ. Press, Oxford, 1997.

9. Shornikova, E. V.; Biadala, L.; Yakovlev, D. R.; Sapega, V. F.; Kusrayev, Y. G.; Mitioglu, A. A.; Ballottin, M. V.; Christianen, P. C. M.; Belykh, V. V.; Kochiev, M. V.; Sibeldin, N. N.; Golovatenko, A. A.; Rodina, A. V.; Gippius, N. A.; Kuntzmann, A.; Jiang, Y.; Nasilowski, M.; Dubertret, B.; Bayer, M. Addressing the exciton fine structure in colloidal nanocrystals: the case of CdSe nanoplatelets. *Nanoscale* **2018**, *10*, 646–656.
10. Pellant, I.; Valenta, J. *Luminescence Spectroscopy of Semiconductors*; Oxford Univ. Press, Oxford, 2012.
11. Achtstein, A. W.; Marquardt, O.; Scott, R.; Ibrahim, M.; Riedl, T.; Prudnikau, A. V.; Antanovich, A.; Owschimikow, N.; Lindner, J. K. N.; Artemyev, M.; Woggon, U. Impact of Shell Growth on Recombination Dynamics and Exciton-Phonon Interaction in CdSe-CdS Core-Shell Nanoplatelets. *ACS Nano* **2018**, *12*, 9476–9483, PMID: 30192515.
12. Ning, Z.; Tian, H.; Qin, H.; Zhang, Q.; Ågren, H.; Sun, L.; Fu, Y. Wave-Function Engineering of CdSe/CdS Core/Shell Quantum Dots for Enhanced Electron Transfer to a TiO<sub>2</sub> Substrate. *J. Phys. Chem. C* **2010**, *114*, 15184–15189.
13. Wang, L.; Nonaka, K.; Okuhata, T.; Katayama, T.; Tamai, N. Quasi-Type II Carrier Distribution in CdSe/CdS Core/Shell Quantum Dots with Type I Band Alignment. *The Journal of Physical Chemistry C* **2018**, *122*, 12038–12046.
14. Ithurria, S.; Tessier, M. D.; Mahler, B.; Lobo, R. P. S. M.; Dubertret, B.; Efros, A. L. Colloidal nanoplatelets with two-dimensional electronic structure. *Nat Mater* **2011**, *10*, 936–941.
15. Cassette, E.; Pensack, R. D.; Mahler, B.; Scholes, G. D. Room-temperature exciton coherence and dephasing in two-dimensional nanostructures. *Nat. Commun.* **2015**, *6*, 7086.